



**HAL**  
open science

## **Dosimetric verification of PENSSART, a new Monte Carlo dose calculation system based on PENELOPE and dedicated to patient-specific treatment quality control in radiotherapy**

Cindy Le Loirec, Juan-Carlos García Hernández, G. Bonniaud, Bénédicte Poumarède, Delphine Lazaro-Ponthus

### **► To cite this version:**

Cindy Le Loirec, Juan-Carlos García Hernández, G. Bonniaud, Bénédicte Poumarède, Delphine Lazaro-Ponthus. Dosimetric verification of PENSSART, a new Monte Carlo dose calculation system based on PENELOPE and dedicated to patient-specific treatment quality control in radiotherapy. Third European Workshop on Monte Carlo Treatment Planning (EWG-MCTP 2012), European Workgroup on Monte Carlo Treatment Planning, May 2012, Sevilla, Spain. cea-02655475

**HAL Id: cea-02655475**

**<https://cea.hal.science/cea-02655475>**

Submitted on 29 May 2020

**HAL** is a multi-disciplinary open access archive for the deposit and dissemination of scientific research documents, whether they are published or not. The documents may come from teaching and research institutions in France or abroad, or from public or private research centers.

L'archive ouverte pluridisciplinaire **HAL**, est destinée au dépôt et à la diffusion de documents scientifiques de niveau recherche, publiés ou non, émanant des établissements d'enseignement et de recherche français ou étrangers, des laboratoires publics ou privés.

# Dosimetric verification of PENSSART, a new Monte Carlo dose calculation system based on PENELOPE and dedicated to patient-specific treatment quality control in radiotherapy

C. Le Loirec<sup>\*1</sup>, J. C. Garcia-Hernandez<sup>1</sup>, G. Bonniaud<sup>2</sup>, B. Poumarède<sup>1</sup> and D. Lazaro<sup>1</sup>

<sup>1</sup> CEA, LIST-DOSEO, F-91191 Gif-sur-Yvette, France

<sup>2</sup> Centre de Médecine Nucléaire du Morbihan, Centre d'Oncologie Saint-Yves, 56000 Vannes, France

## I. Introduction

Beam delivery in radiotherapy has become increasingly complex since the advance of 3D conformational radiotherapy (3DCRT), intensity modulated radiotherapy (IMRT) and stereotactic body radiotherapy (SBRT). With these high precision modalities, accurate dose calculations are essential for radiotherapy planning since the accuracy of the absorbed dose as prescribed determines the clinical outcome.

However, in presence of air cavities or inhomogeneities in the patient anatomy, commercial treatment planning systems (TPSs), in particular those based on the pencil beam algorithm, often fail to predict accurate dose distributions<sup>10</sup>. Systematic errors exceeding 10 % in the thoracic area have been reported.

To further spatially optimize dose distribution, dose calculation algorithms have thus to be improved. Monte Carlo (MC) simulation is the only method that explicitly transports photons and electrons within a material and is therefore likely to provide more accurate results at material interfaces and within inhomogeneities. However, MC methods remain time consuming and their integration into commercial TPS and their use in clinical settings<sup>11, 4</sup> are the result of several improvements, among which implementation of variance reduction techniques and assumptions in the physical models. As a consequence, MC-based calculations engines embedded within TPS could be less accurate than dose calculation engines based on MC general-purpose codes. This has recently motivated the development of several in-house MC based verification tools for routine quality assurance in radiotherapy<sup>17, 14, 9, 7</sup>.

To obtain accurate dose calculations in MC simulations, tissues have to be correctly characterized. Indeed, it has been reported that to overcome significant dose artifacts<sup>3, 16</sup>, it is of prime importance to distinguish between the various densities of lung<sup>1</sup> and also between the various compositions and densities of bone<sup>15</sup>.

In this work, we present a new MC dose calculation system called PENSSART (PENELOPE Simulation for the Safety in Radiotherapy). Prior to dose calculation, we have developed an accurate characterization of biological tissues thanks to a conversion method similar to the one proposed by Vanderstraeten *et al*<sup>15</sup>, based on a stoichiometric calibration method and making used of dosimetrically equivalent tissues subsets. A special attention has been given to bone and lung materials. The schemes obtained for a GE LightSpeed16 scanner have been introduced in PENSSART and validated with a slab phantom.

## II. Materials and Methods

### II.1 Description of the PENSSART system

The PENSSART system is divided into three modules. The dose calculation module is based on the 2006 release of the general-purpose MC code PENELOPE<sup>13</sup> and was designed to perform MC dose calculations within voxelized geometries. It requires as input data a description of the geometry as well as a description of the radiation source, provided by a geometry module and a radiation source module, respectively. The radiation source module is also based on the 2006 release of PENELOPE and allows the simulation of different kinds of radiation sources, going from simple sources such as monoenergetic beams to more complex sources like the one resulting from the complete modeling of a linear accelerator (linac) treatment head. To generate phase space files (PSF) resulting from the complete description of a linac, a new version of the main program PENMAIN was developed, in which several conventional variance reduction techniques (Russian roulette combined with angular splitting, selective bremsstrahlung splitting and rotational splitting) were implemented. Finally, the geometry module was implemented to assist the user in the description of complex geometries (phantoms, patients).

In this work, we will focus on the geometry module and especially on the conversion of DICOM images into MC data.

### II.2 Description of the geometry module

The geometry module has been developed to prepare voxelized geometries in which dose computations will be performed. Two kinds of geometries are supported by the system: *i*) numerical phantoms created using a routine provided in the PENELOPE package which allows the conversion of volumes limited by quadric volumes into voxelized objects and *ii*) voxel-based patient models obtained by converting DICOM images into data usable by the MC dose calculation module. This enables to make direct comparisons between PENSSART and PENELOPE computations and will ease the validation process between the two codes.

A two step procedure has been developed to convert DICOM images into MC data. First, a stoichiometric calibration<sup>8</sup> was used to obtain CT number to density curves. Images of the electron density phantom CIRS Model 062 were used to perform the calibration of a GE LightSpeed16 scanner. In a second step, we used a CT conversion scheme<sup>15</sup> to extract the

\* Author to whom any correspondence should be addressed  
cindy.le-loirec@cea.fr

58 elemental composition data and divide the CT number scale into dosimetrically equivalent tissue subsets (or bins). PENELOPE  
 59 dose calculations were performed with a  $10 \times 10 \text{ cm}^2$  12 MV photon beam produced by a Saturne 43 linac, within  
 60 homogeneous phantoms with dimensions  $31 \times 31 \times 20 \text{ cm}^3$ . The dimensions of the scoring grid voxels were 1 cm in the X  
 61 and Y directions and 0.2 cm in the Z direction. The statistical uncertainty ( $1\sigma$ ) of the MC calculations was less than 0.5 %  
 62 within each voxel of the central axis. For materials between lung and bone, the goal is to keep a deviation less than 1 % for  
 63 each voxel of the central axis within two materials representing adjacent tissue subset. To eliminate the influence of mass  
 64 density, it was set to  $1 \text{ g.cm}^{-3}$  for all these materials. For materials between air and lung, no method was proposed to sample  
 65 the bins. For these materials, mass density is the only factor that influences dose computation as the chemical composition  
 66 keeps the same between adjacent tissue subsets. Under this condition two lung bins have been first defined to allow the  
 67 discrimination between air, inflated lung and deflated lung.

68  
 69 **II.3 Validations**

70 **II.3.1 Dosimetric validation of PENSSART**

71 A first validation benchmark has been conducted to ensure that the PENSSART system gives similar dose results as  
 72 PENELOPE. PENELOPE was already comprehensively validated against dose measurements in previous studies for several  
 73 homogeneous and heterogeneous phantoms<sup>5, 6</sup> and is therefore considered as the reference code in this study. A PSF file  
 74 corresponding to a  $10 \times 10 \text{ cm}^2$  field size for a 12 MV photon beam of a Saturne 43 linac was created at a distance of 100 cm  
 75 from the source, using a linac model previously validated<sup>5</sup>. Dose computations were then performed using this PSF file with  
 76 PENSSART and PENELOPE in a homogeneous water phantom and a layered inhomogeneous phantom.

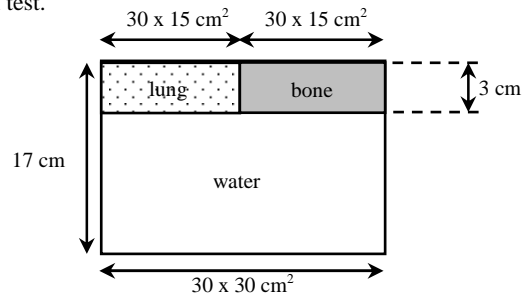
77 To assess the accuracy of the dose computation, we also performed the ICCR00 benchmark<sup>12</sup> for PENELOPE and  
 78 PENSSART. A realistic clinical  $1.5 \times 1.5 \text{ cm}^2$  photon beam is used to irradiate a multi-slab phantom made of the following  
 79 materials: water (from 0 to 3 cm depth), aluminum (from 3 to 5 cm depth), lung (from 5 to 12 cm depth) and water (from 12  
 80 to 30 cm depth). The source is uniform and placed at 100 cm upon the phantom. The 18 MV photon spectrum used is given  
 81 in the benchmark. The PENELOPE energetic parameters used for the dose calculation are in agreement with the EGS4  
 82 parameters given in the benchmark<sup>12</sup>. The depth dose distribution is scored in  $0.5 \times 0.5 \times 0.2 \text{ cm}^3$  voxels.

83  
 84 **II.3.2 Conversion of DICOM images into MC data**

85 Conversion schemes proposed for the GE LightSpeed16 CT scanner were validated for a slab heterogeneous phantom  
 86 described on Figure 1. Four conversion schemes were performed for 140 kV, 120 kV, 100 kV and 80 kV. The slab phantom  
 87 was acquired at 120 kV. To assess the influence of the scanner potential, the four conversion schemes were tested. Dose  
 88 computation was then performed on the 120 kV converted images. The slab phantom was also directly described as a  
 89 numerical phantom in the geometry module, using the exact chemical composition for each material it is made of. The  
 90 comparison between the 3D dose maps computed using the exact geometry of the slab phantom and using the geometry  
 91 obtained after applying the conversion scheme was used as a validation test.

92

Material	Density ( $\text{g.cm}^{-3}$ )	Elemental composition (percentage in mass)
Water	1.00	O (88.89) ; H(11.11)
Lung	0.30	C (60.08) ; O (23.04) ; H (8.33) Mg (4.8) ; N (2.73) ; Cl (1.02)
Bone	1.92	O (43.5) ; Ca (22.5) ; C (15.5) ; P (10.3) ; N (4.2) H (3.4) ; S (0.3) ; Mg (0.2) ; Na (0.1)



93  
 94 **Figure 1:** Slab phantom and materials used to validate the scheme of conversion of CT numbers into MC data.

95  
 96 **III. Results**

97 **III.1 Conversion of DICOM images into MC data**

98 The bin conversion obtained with the method proposed by Vanderstraeten *et al*<sup>15</sup> and with the PENELOPE MC code are  
 99 reported in Table 1. Thirteen bins corresponding to thirteen biological materials were finally determined: among them, seven  
 100 different materials are necessary to accurately describe bony structures for MC dose calculations and two different materials  
 101 are necessary to differentiate lung exhale tissues from lung inhale tissues. This is in contradiction with conversion schemes  
 102 already proposed by other groups who developed quality assurance tools for TPS verification. For example, the  
 103 EGSnrc/DOSXYZnrc default CTCREATE subroutine used in some in-house MC calculations systems<sup>9, 4</sup> assigns only 4  
 104 types of tissues (air, lung, soft tissues and bone). It has been demonstrated that such a coarse segmentation can lead to serious  
 105 errors in the dose computation, up to 10 % for 6 MV photon beams<sup>2</sup>.

106 We have reported on Figure 2 the evolution of the Hounsfield number with the potential for the GE LightSpeed 16 CT.  
 107 We note a large influence of the scanner potential used to make the calibration on the segmentation, especially for bony  
 108 tissues. Indeed, as reported by Verhaegen and Devic<sup>16</sup>, for bony tissues the Hounsfield numbers decrease rapidly with kVp

109 (25 % difference between 80 kVp and 140 kVp) whereas for lung and soft tissues they slightly increase with kVp (5 %  
 110 difference between 80 kVp and 140 kVp).

111 We have then performed a dose computation on the 120 kV converted image. The same dose computation has also been  
 112 performed for a numerical phantom describing the slab phantom with the exact materials. The matching between the two  
 113 dose maps is excellent for the materials considered here (thus compact bone, lung and water). On Figure 3, we have reported  
 114 the profiles obtained at 5 cm depth, thus after the interface between the two inserts (lung and bone) and water.  
 115  
 116

Table 1: Conversion of CT numbers into material composition.

Bin		Composition (masse percentage)											Density ( $g.cm^{-3}$ )	
		H	C	N	O	Na	Mg	P	S	Cl	K	Ca		Ar
1	AIR	-	0.16	78.44	21.08	-	-	-	-	-	-	-	0.33	0.001
2	Lung tissues	10.29	10.16	3.08	75.28	0.20	-	0.20	0.30	0.30	0.20	-	-	0.328
3		10.30	10.18	2.94	75.38	0.20	-	0.20	0.30	0.30	0.20	-	-	0.654
4	Soft tissues	10.76	32.38	2.05	54.04	0.11	-	0.11	0.21	0.21	0.11	-	-	0.816
5		11.07	47.23	1.46	39.78	0.05	-	0.05	0.15	0.15	0.05	-	-	0.978
6		9.98	16.29	4.28	68.38	0.36	-	0.05	0.36	0.25	0.05	-	-	1.073
7	Bony tissues	8.78	21.17	3.89	58.52	0.28	0.04	2.15	0.32	0.18	0.03	4.62	-	1.167
8		7.77	25.32	3.56	50.13	0.21	0.08	3.94	0.29	0.13	0.02	8.56	-	1.261
9		6.90	28.89	3.27	42.91	0.15	0.11	5.48	0.26	0.08	0.01	11.95	-	1.355
10		6.13	32.01	3.02	36.61	0.10	0.13	6.82	0.23	0.03	-	14.91	-	1.449
11		4.58	22.60	3.69	40.54	0.10	0.17	8.80	0.27	0.01	-	19.23	-	1.68
12		3.95	18.82	3.96	42.12	0.10	0.19	9.60	0.29	-	-	20.97	-	1.80
13		3.40	15.50	4.20	43.50	0.10	0.20	10.30	0.30	-	-	22.50	-	1.92

117  
 118  
 119  
 120  
 121  
 122  
 123  
 124  
 125  
 126  
 127  
 128  
 129

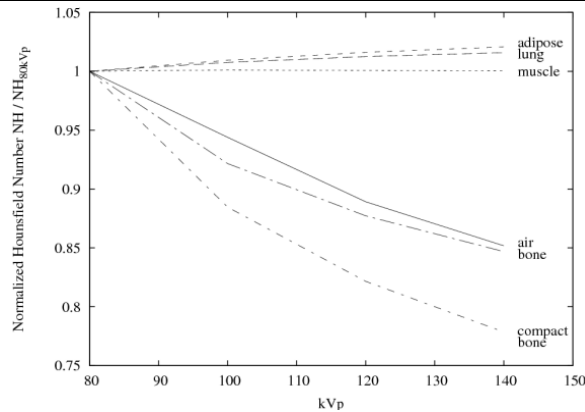


Figure 2: Evolution of Hounsfield numbers with the scanner potential for the GE LightSpeed16 CT.

130  
 131  
 132  
 133  
 134  
 135  
 136  
 137  
 138  
 139  
 140  
 141  
 142  
 143  
 144  
 145  
 146  
 147  
 148

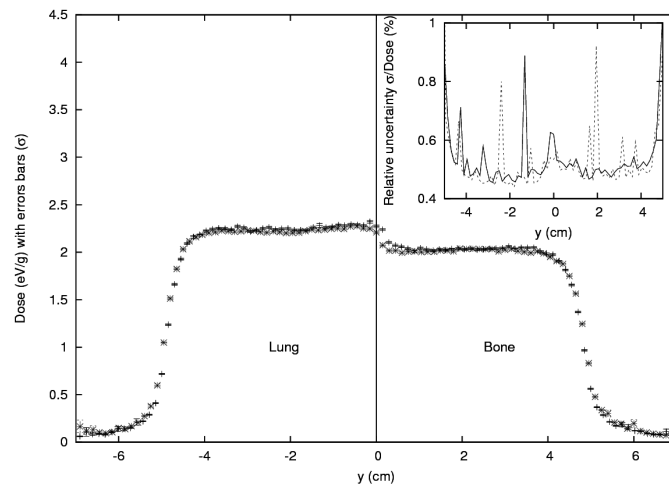


Figure 3: Profiles obtained at 5.0 cm depth. Solid line and “+” crosses correspond to the dicom image and dash line and “x” crosses correspond to the exact slab geometry.

149 *III.2 Dosimetric validation of PENSSART*

150 For the three benchmarks performed, the standard deviation between PENELOPE and PENSSART is less than 2 % except  
151 at the interface between lung and water and also for the depths where an uncertainty higher than 2 % is observed for one of  
152 the two codes. The build-up computed by PENSSART at the interface between lung and water is moved compared to the one  
153 computed by PENELOPE. This difference is due to the fact that dose computation is performed in a voxelized geometry in  
154 PENSSART whereas it is performed in a quadratic geometry in PENELOPE.

155 Relative depth dose distributions computed with PENELOPE, PENSSART and EGS4 for the ICCR00 have been also  
156 performed for 100 millions of particles in the conditions specified by the benchmark <sup>12</sup>. A good agreement between the three  
157 codes is observed for the depth dose distributions. Nevertheless, some discrepancies appear at the interfaces between  
158 heterogeneities: it was observed that PENELOPE and PENSSART both underestimate the lung dose compared to EGS4. At each  
159 interfaces, large deviations comprised between 5 and 10 % can be noted. Out of these interfaces, the deviation between the  
160 codes is comprised between  $\pm 2$  %.

161  
162 **IV. Conclusions**

163 Development of the PENSSART system was successful for performing MC simulations in heterogeneous media. We have  
164 presented here the key features of the system. A CT conversion scheme has been developed whereby a material can be  
165 assigned to each voxel of a DICOM image. Materials have been chosen in such way that the doses obtained by MC  
166 calculations are not expected to differ by more than one percent from the doses obtained with the real tissues. Investigations  
167 are currently driven to precise this conversion scheme in the case of pulmonary SBRT treatments.

168 The next step will be to adapt the PENSSART system for quality control of IMRT treatment plans in radiotherapy. To this  
169 end, developments are already on-going: models of the Siemens ARTISTE linac and its 160 MLC<sup>TM</sup> were already validated  
170 and clinical cases will be tested in the future months with the PENSSART system.

171  
172 **References**

173 <sup>1</sup> Aarup L R et al 2009 The effect of different lung densities on the accuracy of various radiotherapy dose calculation  
174 methods: implications for tumour coverage *Radiotherapy and Oncology* **91** 405-414  
175 <sup>2</sup> Bazalova M 2008, The use of computed tomography images in Monte Carlo treatment planning, PhD thesis (McGill  
176 University, MONTREAL, QUEBEC)  
177 <sup>3</sup> Du Plessis F C P, Willemse C A and Lötter M G 1998 The indirect use of CT numbers to establish material properties  
178 needed for Monte Carlo calculation of dose distributions in patients *Med. Phys.* **25** 1195-1201  
179 <sup>4</sup> Gardner J and Siebers J 2007 Dose calculation validation of VMC++ for photon beams *Med. Phys.* **34** 1809-1818  
180 <sup>5</sup> Habib B, Poumarede B, Tola F and Barthe J 2010, Evaluation of PENFAST – A fast Monte Carlo code for dose calculations  
181 in photon and electrons radiotherapy treatment planning, *Phys. Med.* **26** 17-25  
182 <sup>6</sup> Lazaro-Ponthus D, Guérin L, Batalla A, Frisson T and Sarrut D 2011, Commissioning of PENELOPE and GATE Monte  
183 Carlo models for 6 and 18 MV photon beams from the Siemens Artiste linac, 11<sup>th</sup> Biennial ESTRO, London UK  
184 <sup>7</sup> Ma C-M et al 2002 A Monte Carlo dose calculation tool for radiotherapy treatment planning *Phys. Med. Biol.* **47** 1671-1689  
185 <sup>8</sup> Martinez L C et al 2011 A parametrization of the CT number of a substance and its use for stoichiometric calibration  
186 *Physica Medica in press*  
187 <sup>9</sup> Mukumoto N et al 2009 A preliminary study of in-house Monte Carlo simulations: an integrated Monte Carlo verification  
188 system *Int. J. Radiation Oncology Biol. Phys.* **75** 571-579  
189 <sup>10</sup> Papanikolaou N and Stathakis S 2009 Dose calculation algorithms in the context of inhomogeneity corrections for high  
190 energy photon beams *Med. Phys.* **36** 4765-4774  
191 <sup>11</sup> Reynaert N et al 2007 Monte Carlo treatment planning for photon and electron beams *Radiation Physics and Chemistry*  
192 **76** 643-686  
193 <sup>12</sup> Rogers D W O and Mohan M 2000 Questions for comparison of clinical Monte Carlo code in *Proc. ICCR 2000*  
194 <sup>13</sup> Salvat F, Fernández-Varea J M and Sempau J 2006 PENELOPE—A code system for Monte Carlo simulation of electron  
195 and photon transport *OECD Nuclear Energy Agency Issy-les-Moulineaux France*  
196 <sup>14</sup> Tang F, Sham J, Ma C-M and Li J-S 2007 Monte Carlo – based QA for IMRT of head and neck cancers *Journal of*  
197 *Physics : Conference Series* **74** 012021  
198 <sup>15</sup> Vanderstraeten B et al 2007 Conversion of CT numbers into tissue parameters for Monte Carlo dose calculations: a multi-  
199 centre study *Phys. Med. Biol.* **52** 539-562  
200 <sup>16</sup> Verhaegen F and Devic S 2005 Sensitivity study for CT image use in Monte Carlo treatment planning *Phys. Med. Biol.*  
201 **50** 937-946  
202 <sup>17</sup> Yamamoto T et al An integrated Monte Carlo dosimetric verification system for radiotherapy treatment planning 2007  
203 *Phys. Med. Biol.* **52** 1991-2008